Journal of Luminescence 134 (2013) 107–112

Contents lists available at SciVerse ScienceDirect

Journal of Luminescence

journal homepage: www.elsevier.com/locate/jlumin

Optical and electrical properties of electrochemically doped organic field effect transistors

Cigdem Yumusak [a,b,*], Mamatimin Abbas [b,1], Niyazi Serdar Sariciftci [b]

[a] Department of Physics, Faculty of Arts and Sciences, Yildiz Technical University, Davutpasa Campus, Esenler, 34210 Istanbul, Turkey
[b] Linz Institute for Organic Solar Cells (LIOS), Physical Chemistry, Johannes Kepler University of Linz, A-4040 Linz, Austria

ARTICLE INFO

Article history:
Received 22 May 2012
Received in revised form
28 August 2012
Accepted 5 September 2012
Available online 16 September 2012

Keywords:
Organic light emitting transistor
Organic field effect transistor
Electrochemical transistor
Electrochemical light emitting transistor
Electrochemical doping
Organic electronics

ABSTRACT

Mixed ionic/electronic conduction in conducting polymers introduces new physics/chemistry and an additional functionality in organic optoelectronic devices. The incorporation of an ionic species in a conjugated polymer matrix results in the increase in electrical conductivity associated with the electrochemical doping of the material. In recent years polymer light emitting electrochemical cells (LECs) have been demonstrated. In such electrochemical optoelectronic devices, mobile ions facilitate the efficient injection of electronic charge carriers creating "*in situ*" doping regions near the electrodes and lead to efficient electroluminescence light emission. Here, we introduce the same concept of an LEC in the organic field effect transistors (OFETs). The presence of both electronic and ionic charge carriers in the active layers of OFETs brings high charge carrier mobility and light emission even using symmetric source and drain metal electrodes.

1. Introduction

Conjugated polymers have attracted great attention since the discovery of electrical conductivity in chemically doped polyacetylene [1], because they combine the electrical and optical properties of semiconductors with the processing advantages of polymers. Potential applications are in the fields of organic light emitting diodes (OLEDs) [2,3], organic solar cells [4] (OPV), organic field effect transistors (OFETs) [5–7], biosensors [8], and electrochromic devices [9]. Using conjugated polymers to fabricate optoelectronic devices is attractive due to their low production cost (roll-to-roll production possibility), processability from solution,and mechanical as well as chemical structural flexibility by modifying their optical and electronic properties through chemical modifications.

Electroluminescence organic diodes (OLEDs) were first discovered by Tang and VanSlyke [2]. Using conjugated polymers in OLEDs was first reported in poly(*para*-phenylene vinylene) (PPV) in 1990 [3]. Since then considerable effort has been devoted to developing conjugated polymeric materials as the active units in light emitting devices for use in display applications. Small molecular OLED based displays and lighting fixtures are already released to the market. OFETs have been developed as switching devices for active matrix LCD and LED displays [10,11]. Because the electroluminescent intensity of OLEDs is controlled by the current density, at least two organic transistors are necessary for a complete driving pixel of active matrix LEDs. Therefore, the driving circuits are usually obtained by complicated fabrication techniques, which increase the cost dramatically.

On the other hand, organic light emitting field effect transistors (OLEFETs) represent a significant technological advance by combining two functionalities –electrical switching and light emission – in a single device, thus significantly increasing the potential applications of conjugated polymers [12–16]. In particular, if appropriate materials and device structures can be introduced, OLEFETs offer an ideal alternative to organic light-emitting heterostructures due to the intrinsically different driving conditions and charge-carrier balance of OFETs as compared to conventional OLEDs. Due to this unique combination of properties, OLEFETs have potential in the fabrication of simplified pixels in flat panel displays, highly integrated optoelectronic devices in communications, sensors, and electrically driven organic displays and lasers [17–23].

OFETs have been fabricated with various device geometries [24]. Fig. 1 illustrates an OFET structure with bottom gate/bottom contact geometry. The working principle of an OLEFET is based on the simultaneous injection of electrons and holes into a double or

* Corresponding author at: Yildiz Technical University, Department of Physics, Faculty of Arts and Sciences, Davutpasa Campus Esenler, 34210 Istanbul, Turkey. Tel.: +90 212 3834258; fax: +90 212 3834234.
E-mail addresses: yumusak@yildiz.edu.tr, cyomega@gmail.com (C. Yumusak).
[1] Present Address: Laboratoire IMS, Universite Bordeaux 1, UMR 5218 CNRS, ENSCBP, 16 Avenue Pey-Berland, 33607 Pessac Cedex, France.

0022-2313/$ - see front matter © 2012 Elsevier B.V. All rights reserved.
http://dx.doi.org/10.1016/j.jlumin.2012.09.003

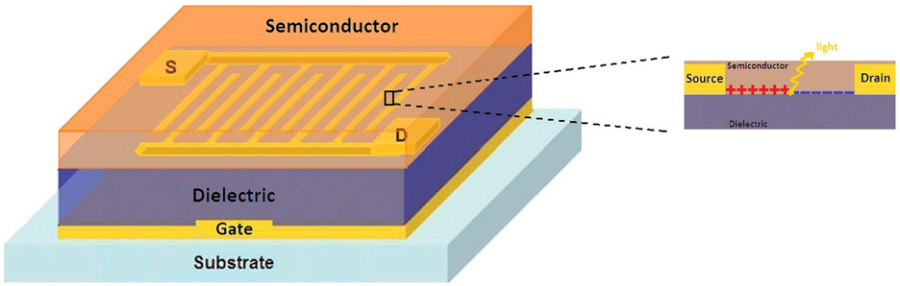

Fig. 1. Schematic diagram of bottom gate/bottom contact OFET structure. The inset shows light emission from a light emitting field effect transistor.

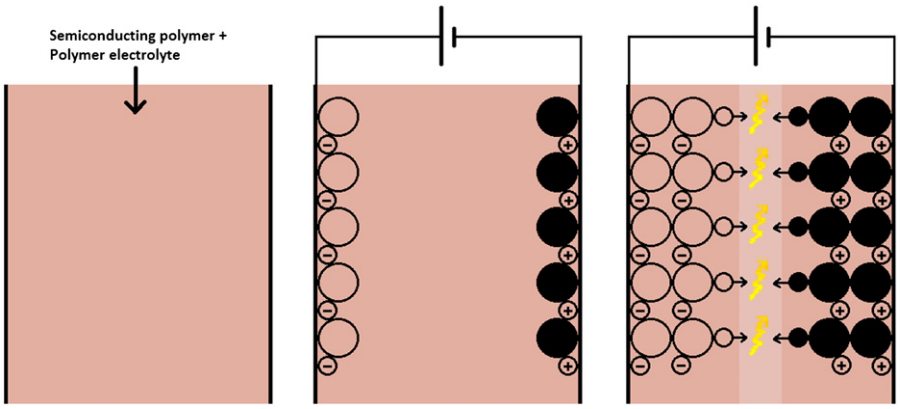

Fig. 2. Schematic diagram of the electrochemical processes in a light emitting electrochemical cell.

ambipolar layer by tuning of the gate–source and drain–source voltages. The accumulated charge is zero when the biasing conditions are such that the potential at some point in the channel equals the gate potential. Consequently, at this point the electron and hole accumulation layers vanish (Fig. 1). Exciton formation occurs near this point and radiative relaxation of these excitons to the ground state leads to light emission. Although the basic concept of an OLEFET dates back to 1996 [25], the development of OLEFETs is still in a relatively early stage.

The first OLEFET has been demonstrated by Hepp et al. [26] and is based on vacuum-evaporated tetracene as the organic semiconductor. Since this first demonstration, OLEFETs have been fabricated using polymers [27,28], small molecules [29–31], a heterostructure of *p*- and *n*-type organic semiconductors [32–37] and the ambipolar polymeric semiconductors [38,39]. Recently, Muccini et al. reported high external quantum efficiency of 5% using a trilayer heterostructure device composed of a light emitting layer sandwiched between *p*-type and *n*-type layers [40].

The conjugated polymers used in OLEFETs should possess both excellent field effect mobility and good light emitting characteristics. In order to achieve high conductivity, conjugated polymers can be doped by chemical [41–43] or electrochemical mechanisms [43–45]. On the other hand, electrostatic field induced doping of conjugated polymers has been widely reported in the context of organic filed effect transistors [46,47]. In contrast to chemical and electrochemical doping experiments, carrier density in field effect transistor devices is determined by the gate voltage induced charge density.

To enhance the field effect induced doping, several groups have also demonstrated that solution processable solid polymer electrolytes, such as polyethylene oxide (PEO) with dissolved Li salts, can be used as gate insulator materials in transistors [48–53].

In principle, there are two basic mechanisms by which electrolyte–gated transistors can operate. Upon application of a gate voltage, an electrical double layer forms at the gate/electrolyte interface. At the semiconductor/electrolyte interface a second double layer can form composed of accumulated carriers in the semiconductor and oppositely charged ions in the electrolyte. This is the "electrostatic doping" or field effect regime. In some cases, ions from the electrolyte do not penetrate the semiconductor. Alternatively, if the semiconductor is permeable (which can be easily the case with polymeric semiconductors), ions from the polymer electrolyte dielectric will cross the semiconductor/electrolyte interface and penetrate into the semiconductor. In this case, charges (e.g., holes) accumulated in the semiconductor are balanced by the diffusion of counterions (e.g., anions). This is the electrochemical doping regime, which was well-established in experiments on microelectro-chemical transistors in the 1980s [54–56].

The effect of ions on the generation and transport of charge carriers in semiconductors is not an unfamiliar concept; the first demonstration of the sensitivity of a Si transistor in an ionic solution was reported more than 40 years ago [57]. Furthermore, in recent years polymer light emitting electrochemical cells (LECs) have been demonstrated, in which mobile ions facilitate the efficient injection of electrons and holes into luminescent organic semiconductors by doping the semiconducting polymer in *p* and *n*-type near the anode and cathode, respectively [58].

Polymer LECs are novel polymer light-emitting devices operating on the principle of "*in situ*" electrochemical doping, basically distinct from OLEDs which are based on the intrinsic properties of undoped semiconducting polymers. LECs consist of a polymer blend containing a luminescent conjugated polymer, an ion conductive polymer and an ionic salt sandwiched between an indium tin oxide (ITO) electrode and a metal electrode. When the applied bias is greater than the energy gap of the luminescent polymer, the ions dissociated from the salt dope the conjugated polymer *p*-type near the anode and *n*-type near the cathode, and a *p*–*i*–*n* junction is formed "in situ" by electrochemical doping during the biasing (Fig. 2).

Anode reaction:

$$(\pi-\text{polymer})+[D^+A^-]_{solv}\rightarrow[(\pi-\text{polymer})^{x+}(A^-)_x]+xD^++xe^- \quad (1)$$

Cathode reaction:

$$(\pi-\text{polymer})+xe^-+[D^+A^-]_{solv}\rightarrow[(\pi-\text{polymer})^{x-}(D^+)_x]+x(A^-) \quad (2)$$

where D^+A^- is the salt in the electrolyte. The doping near the metallic electrodes facilitates charge injection, holes into *p*-type doped material and electrons into *n*-type doped material. As sketched in Fig. 2, light emission occurs in the intrinsic region between the *p*- and *n*-doped layers where the opposite charge carriers recombine radiatively [58–63].

To use the same ideology of an LEC in the OFETs can lead to new features and functionality [64,65]. Because of the mixed ionic/electronic conduction mechanisms in conjugated polymers –conjugated polyelectrolyte composites, additional functionalities can be introduced [66]. These materials combine the electronic and optical qualities of conjugated polymers with the properties of polyelectrolytes and all this can be modified by applied gate voltages [66–68].

Here we report doped OFETs consisting of a conjugated luminescent polymer poly[2-methoxy-5-(3',7'-dimethyloctyloxy)–1,4-phenylenevinylene] (MDMO–PPV) mixed with polymer electrolyte poly(ethylene oxide) (PEO) including lithium trifluoromethanesulfonate ($LiCF_3SO_3$) as an active layer and benzocyclobutane (BCB) as a gate dielectric. The role of ionic charge carriers in the active layers of OFETs have been demonstrated by investigating detailed optoelectronic characteristics.

2. Experimental methods

2.1. Device fabrication

OFETs were fabricated using transparent ITO coated glasses as gate electrode/substrate. ITO coated glass substrates 15×15 mm^2 were etched, leaving an area of 5×15 mm^2 as a gate electrode and cleaned using acetone, 2-propanol, Hellmanex glass cleaning solution, and finally with deionized H_2O in an ultrasonic bath. Benzocyclobutene (BCB) purchased from Dow Chemicals was spin coated on top of the ITO substrate as a transparent gate dielectric (Fig. 1). The area of the BCB gate dielectric was optimized by removing the thin film with the mesitylene solvent and subsequently cured at 260 °C for 2 h in a vacuum oven. The average thickness of the dielectric was about 1–1.5 μm. Measured dielectric capacitance in inert condition with the thickness of the dielectric layer consistently gave the values of the dielectric constant ε of 2.6 and capacitance C_i of 1.3 nF/cm^2. Following the BCB curing, bottom contact source and drain electrodes consisting of 60 nm Au were evaporated under high vacuum ($\sim10^{-6}$ Torr) through a shadow mask. The channel length (L) and the channel width (W) of the device was 30 μm and 5 mm, respectively. The conjugated polymer MDMO–PPV and the polymer electrolyte consisted of poly(ethylene oxide) (PEO) and lithium trifluoromethanesulfonate (Li triflate) were obtained from Sigma-Aldrich Co. MDMO–PPV, PEO, and Li triflate were blended 5:5:1 by weight and dissolved in pyridine to create master solutions of concentrations of 1% (w/v).

2.2. Device characterization

Steady state current–voltage measurements were performed at room temperature using an Agilent E5273A parametric analyzer with two source-measure units and the light emission intensity was simultaneously detected by a photomultiplier placed just above the device. Keithley 236 source-measure unit instrument was also employed to take the light output. All measurements were performed at a scan rate of 1 V/s. The electroluminescence spectra were recorded by a calibrated spectrophotometer (Spectra Scan PR-655, Photo Research, CA). Photoluminescence measurements were performed with a Horiba Yobin Ivon Fluorolog-3 spectrafluorometer. The spatial distribution of light emission of the operating device was taken by a digital camera through an optical microscope. Both device fabrication and characterization were performed in a glovebox under nitrogen atmosphere with <1 ppm water and oxygen content.

3. Results and discussion

Fig. 3 shows the output characteristics of the doped and the undoped OFETs. The drain–source voltage V_{DS} is swept from 0 to –60 V, while the gate–source voltage V_{GS} is changed stepwise from 0 to –60 V in 15 V steps. It is evident from Fig. 3 that the devices exhibit the *I–V* characteristics of unipolar OFETs with saturation behavior and therefore the OFETs operate in the hole accumulation mode. There are two main differences between the doped and the undoped devices: the light emission is only detected only from the doped devices and the drain–source current I_{DS} of the doped devices (Fig. 3a) is almost four orders of magnitude higher those of than the undoped devices (Fig. 3b) under the same experimental conditions.

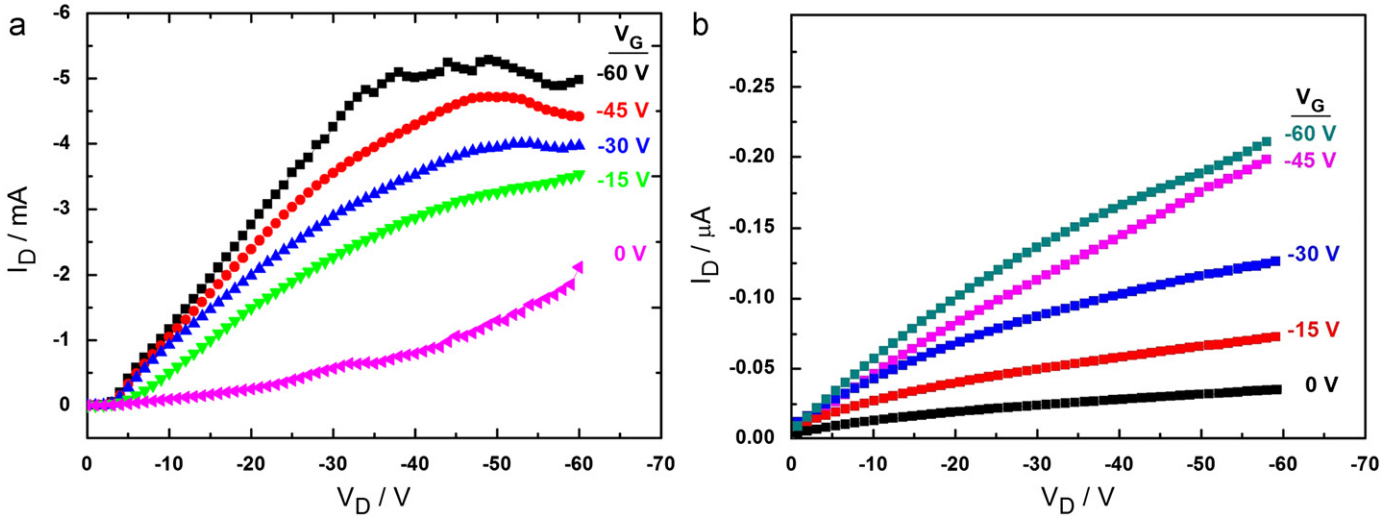

Fig. 3. Electrical output characteristics of the OFETs at various gate voltages (a) doped OFET and (b) undoped OFET.

The optical output characteristics at different gate voltages of the doped devices are shown in Fig. 4. It can be seen that the optical output does not directly follow the current. At a fixed V_{GS}, light emission intensity increases with the increase of V_{DS}. Fig. 5 shows the light intensity as a function of the drain-source current I_{DS} which is recorded by sweeping the drain–source voltage at various constant gate–source voltages.

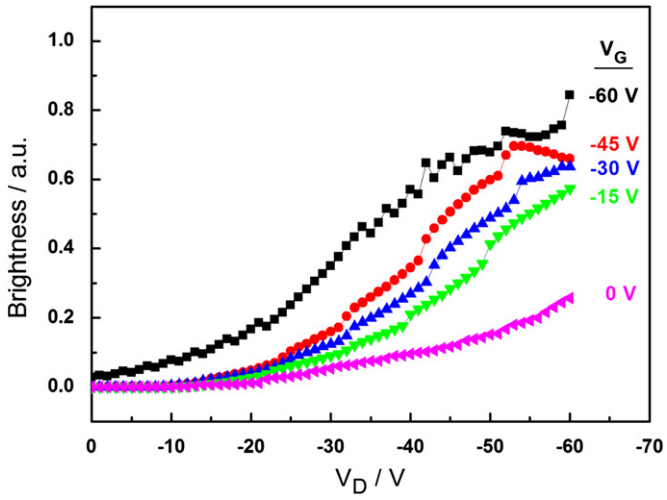

Fig. 4. Optical output characteristics of the doped OFET simultaneously measured with electrical output characteristics.

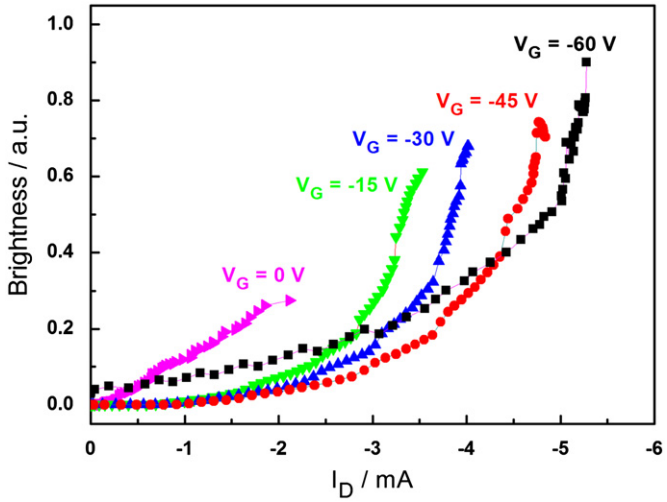

Fig. 5. Light emission intensity vs drain current for different constant gate voltages.

But interestingly, the light emission is not observed in the first sweeps in the doped devices. After several repetitions, the light emission is observed in the saturation regime. On further sweeping cycles, the light emission was observed even from linear regions. Moreover in each next sweeping turn, the doped devices are operating at lower and lower voltages indicating that the injection barrier is going down via consecutive doping near the electrodes. All these show that during operation of the electrochemical OLEFET devices there is a continued "*in situ*" doping and increase in the conductivity occurring. When a negative gate voltage is applied, positive charges are induced at the interface between the active layer and the dielectric layer. The holes are injected from the source electrode and transferred through the channel to the drain electrode. At sufficient drain voltages, electrons are also injected into the active layer from the drain electrode, which results in carrier recombination and light emission. Because of the presence of the electrolyte in the active layer of the doped device, MDMO–PPV gets electrochemically doped at the opposite electrodes and the light emission can be observed at lower voltages even using symmetric Au source and drain electrodes.

Fig. 6a shows the transfer characteristics of a doped OFET along with simultaneously measured light emission intensity data. Fig. 6b shows the transfer characteristics of an undoped OFET as comparison (no light emission is detected while sweeping the gate–source voltage). I_{DS} is measured keeping the drain–source voltage constant at -40 V, while sweeping the gate–source voltage from 0 to –60 V in 1 V steps. Note the close correspondence of both the channel current and the emitted light intensity vs gate voltage. Fig. 6a indicates that the gate bias controls not only the current flow but also the light intensity. The light intensity increases with the gate voltage. On the other hand, the doped device exhibits high field effect hole mobility of about 3 $cm^2 V^{-1} s^{-1}$ calculated in the linear regime using the standard transistor equation [69] whereas hole mobility of the undoped device (standard OFET) is calculated to be $\sim 10^{-3}$ $cm^2 V^{-1} s^{-1}$ which is three orders of magnitude lower than that of the doped device.

Fig. 7 shows the light intensity as a function of I_{DS} which is recorded by sweeping the gate voltage at a constant drain voltage as in Fig. 6a. The light output is directly proportional to the drain current, too.

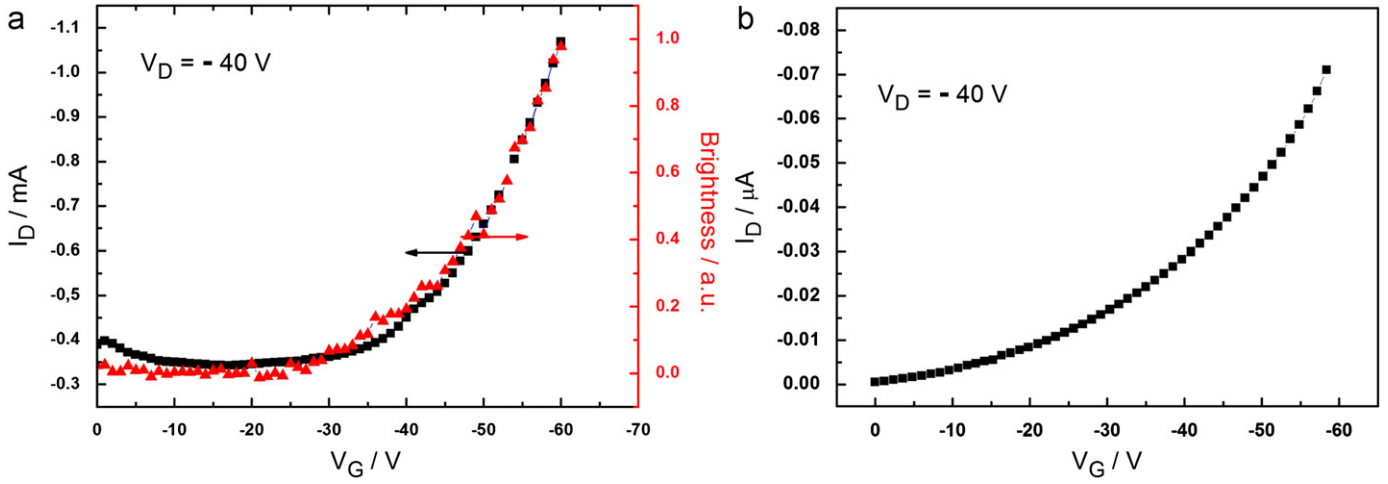

Fig. 6. Electrical transfer characteristics of the OFETs. (a) Electrical transfer characteristics of the doped OFET and simultaneously recorded light emission; the gate voltage was scanned from 0 to -60 V while keeping the drain voltage at a fixed value of -40 V. (b) undoped OFET.

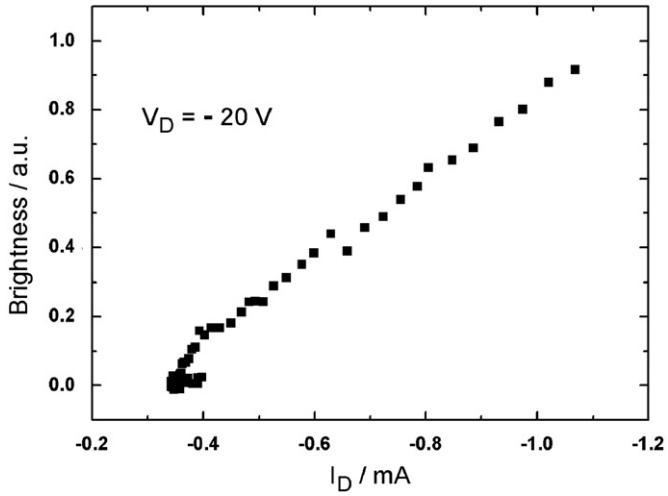

Fig. 7. Light emission intensity vs drain current for a constant drain voltage.

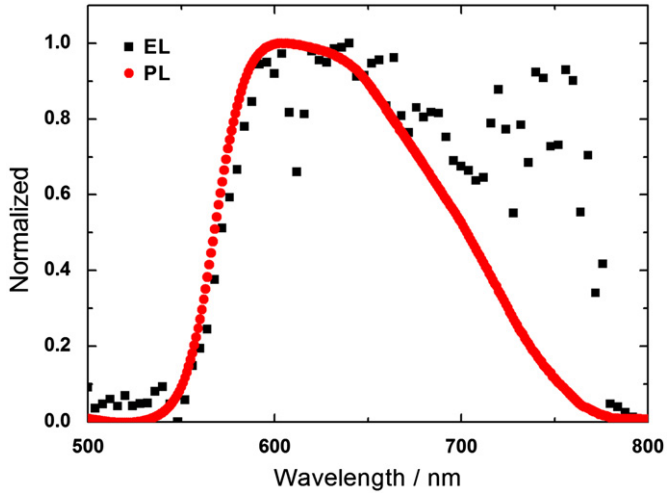

Fig. 8. Normalized EL and PL spectra of the doped OFET.

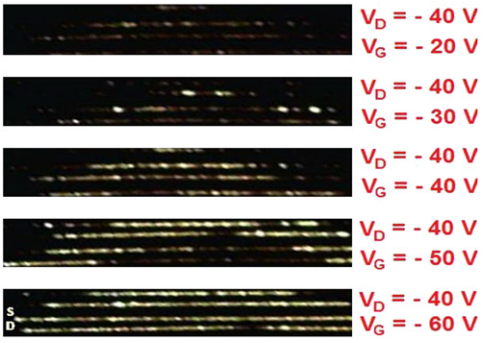

Fig. 9. Spatial distribution of light emission of the operating doped OFET at constant drain voltage and different gate voltages taken through a digital microscope.

The normalized electroluminescence (EL) and photoluminescence (PL) spectra of the doped device are shown in Fig. 8. There is an EL spectrum peak at the wavelength of ca. 600 nm, corresponding to the position of the PL spectrum peak. This peak indicates that emission originates from the intrinsic luminescence of the active MDMO–PPV layer. On the other hand, another EL peak appeared at a longer wavelength of ca. 750 nm, possibly due to polaronic effects of doping (polaron-exciton).

The doped OLEFET emits orange–yellow light which could be seen with the naked eye. Light emission is observed adjacent to the negative biased electrode, which we assign as the drain (D) electrode. This region of emission indicates the charge carrier recombination zone close to the cathode. It is conceivable since the electron mobility is much smaller than the hole mobility in such devices, bringing the statistical recombination zone near to the electron injecting electrode (drain). A series of pictures were taken with constant source–drain bias (V_{DS}) and increasing gate bias (Fig. 9). One realizes that the emission is inhomogeneous and occurs close to the drain electrode.

4. Conclusion

We have studied electrochemically doped OFET devices based on a conjugated polymer MDMO–PPV mixed with polymer electrolyte PEO including Li triflate salt as an active layer and BCB as an insulating layer. The devices exhibit unipolar OFET characteristics and operate in the hole accumulation mode. The hole mobility is obtained as 3 $cm^2\,V^{-1}\,s^{-1}$ which is three orders of magnitude higher than that of the undoped devices. Besides high charge carrier mobility, the doped OFETs exhibit light emission property that is important in light–emitting device technology. The electroluminescence from the operating device is localized close to the electron injecting electrode. The drain voltages and the gate voltages control the light emission intensity. The overall stability of such PPV based devices is low. Optimization of both device architecture and the active layer including solid electrolyte may lead to further improvements in stability and performance. New materials with improved stability and efficiency should be introduced as in the generations of OLEDs during the last 15 years.

Acknowledgements

The authors thank Jacek Gasiorowski, Philipp Stadler and Christoph Ulbricht for fruitful discussions and suggestions. The work was financially supported by the Austrian Science Foundation (FWF Project S 9711-N20). C. Yumusak also gratefully acknowledges the financial support of European Science Foundation (ESF Organisolar Project) for her scientific visit to Linz Institute for Organic Solar Cells (LIOS).

References

[1] C.K. Chiang, C.R. Fischer, Y.W. Park, A.J. Heeger, H. Shirakawa, E.J. Louis, S.C. Gau, A.G. MacDiarmid, Phys. Rev. Lett. 39 (1977) 1098.
[2] (a) C.W. Tang, S.A. VanSlyke, Appl. Phys. Lett. 51 (1987) 913;
(b) S.A. VanSlyke, C.H. Chen, C.W. Tang, Electroluminescence device with organic luminescent medium, US Patent No. 4, 720, 432 1988.
[3] J.H. Burroughes, D.D. Bradley, A.R. Brown, R.N. Marks, K. Mackay, R.H. Friend, P.L. Burn, A.B. Holmes, Nature 347 (1990) 539.
[4] C.W. Tang, Appl. Phys. Lett. 48 (1986) 183.
[5] G. Horowitz, D. Fichou, X. Peng, Z. Xu, F. Garnier, Solid State Commun. 72 (1989) 381.
[6] H. Sirringhaus, N. Tessler, R.H. Friend, Science 280 (1998) 1741.
[7] A. Dodabalapur, Z.N. Bao, A. Makhija, J.G. Laquindanum, V.R. Raju, Y. Feng, H.E. Katz, J. Rogers, Appl. Phys. Lett. 73 (1998) 142.
[8] D.T. McQuade, A.E. Pullen, T.M. Swager, Chem. Rev. (Washington, DC 100 (2000) 2537.
[9] G. Sonmez, Chem. Commun. (2005) 5251, Cambridge.
[10] G. Horowitz, Adv. Mater. 10 (1998) 365.
[11] 〈http://www.vdma.org/oe-a〉.
[12] J.S. Swensen, C. Soci, A.J. Heeger, Appl. Phys. Lett. 87 (2005) 253511.
[13] M. Muccini, Nat Mater 5 (2006) 605.
[14] C.V. Hoven, A. Garcia, G.C. Bazan, T.Q. Nguyen, Adv. Mater. 20 (2008) 3793.

[15] J.H. Seo, G. Andrea, B. Walker, S. Cho, A. Garcia, R. Yang, T.Q. Nguyen, A.J. Heeger, G.C. Bazan, J. Am. Chem. Soc. 131 (2009) 18220.
[16] J.H. Seo, E.B. Namdas, A. Gutacker, A.J. Heeger, G.C. Bazan, Appl. Phys. Lett. 97 (2010) 043303.
[17] T. Sakanoue, E. Fujiwara, R. Yamada, H. Tada, Appl. Phys. Lett. 84 (2004) 3037.
[18] J.S. Swensen, J. Yuen, D. Gargas, S.K. Buratto, A.J. Heeger, J. Appl. Phys. 102 (2007) 013103.
[19] J. Zaumseil, C.L. Donley, J.S. Kim, R.H. Friend, H. Sirringhaus, Adv. Mater. 18 (2006) 2708.
[20] E.B. Namdas, J.S. Swensen, P. Ledochowitsch, J.D. Yuen, D. Moses, A.J. Heeger, Adv. Mater. 20 (2008) 1321.
[21] E.B. Namdas, P. Ledochowitsch, J.D. Yuen, D. Moses, A.J. Heeger, Appl. Phys. Lett. 92 (2008) 183304.
[22] T. Takenobu, S.R. Bisri, T. Takahashi, M. Yahiro, C. Adachi, Y. Iwasa, Phys. Rev. Lett. 100 (2008) 066601.
[23] E.B. Namdas, M. Tong, P. Ledochowitsch, S.R. Mednick, J.D. Yuen, D. Moses, A.J. Heeger, Adv. Mater. 21 (2009) 799.
[24] Th.B. Singh, N.S. Sariciftci, Ann. Rev. of Mate. Res. (2006) 199.
[25] A. Dodabalapur, H.E. Katz, L. Torsi, Adv. Mater. 8 (1996) 853.
[26] A. Hepp, H. Heil, W. Weise, M. Ahles, R. Schmechel, H. von Seggern, Phys. Rev. Lett. 91 (2003) 157 406.
[27] M. Ahles, A. Hepp, R. Schmechel, H. von Seggern, Appl. Phys. Lett. 84 (2004) 428.
[28] J. Swensen, D. Moses, A.J. Heeger, Synth. Met. 153 (2005) 53.
[29] T. Oyamada, H. Uchiuzou, S. Akiyama, Y. Oku, N. Shimoji, K. Matsushige, H. Sasabe, C. Adachi, J. Appl. Phys. 98 (2005) 074.
[30] J. Reynaert, D. Cheyns, D. Janssen, R. Müller, V.I. Arkhipov, J. Genoe, G. Borghs, P. Heremans, J. Appl. Phys. 97 (2005) 114.
[31] C. Santato, R. Capelli, M.A. Loi, M. Murgia, F. Cicoira, V.A.L. Roy, P. Stallinga, R. Zamboni, C. Rost, S.F. Karg, M. Muccini, Synth. Met. 146 (2004) 329.
[32] C. Rost, S. Karg, W. Rieß, M.A. Loi, M. Murgia, M. Muccini, Appl. Phys. Lett. 85 (2004) 1613.
[33] C. Rost, S. Karg, W. Rieß, M.A. Loi, M. Murgia, M. Muccini, Synth. Met. 146 (2004) 237.
[34] M.A. Loi, C. Rost, M. Murgia, S. Karg, W. Rieß, M. Muccini, Adv. Funct. Mater. 16 (2006) 41.
[35] F. Dinelli, R. Capelli, M.A. Loi, M. Muccini, A. Fachetti, T.J. Marks, Adv. Mater. 18 (2006) 1416.
[36] R. Capelli, F. Dinelli, M.A. Loi, M. Murgia, R. Zamboni, M. Muccini, J. Phys.: Condens. Matter 18 (2006) S2127.
[37] S. De Vusser, S. Schols, S. Steudel, S. Verlaak, J. Genoe, W.D. Oosterbaan, L. Lutsen, D. Vandezande, P. Heremans, Appl. Phys. Lett. 89 (2006) 223.
[38] J. Zaumseil, R.H. Friend, H. Sirringhaus, Nat. Mater. 5 (2006) 69.
[39] J. Zaumseil, C.L. Donley, J. Kim, H. Friend, H. Sirringhaus, Adv. Mater. 18 (2006) 2708.
[40] R. Capelli, S. Toffanin, G. Generali, H. Usta, A. Facchetti, M. Muccini, Nat. Mater. 9 (2010) 496.
[41] C.K. Chiang, C.R. Fincher Jr., Y.W. Park, A.J. Heeger, H. Shirakawa, E.J. Louis, S.C. Gau, A.G. MacDiarmid, Phys. Rev. Lett. 39 (1977) 1098.
[42] M. Reghu, Y. Cao, D. Moses, A.J. Heeger, Phys. Rev. B 47 (1993) 1758.
[43] R.S. Kohlman, A. Zibold, D.B. Tanner, G.G. Ihas, T. Ishiguro, Y.G. Min, A.G. MacDiarmid, A.J. Epstein, Phys. Rev. Lett. 78 (1997) 3915.
[44] K. Lee, E.K. Miller, A.N. Aleshin, R. Menon, A.J. Heeger, J.H. Kim, C.O. Yoon, H. Lee, Adv. Mater. 10 (1998) 456.
[45] I.N. Hulea, H.B. Brom, A.J. Houtepen, D. Vanmaekelbergh, J.J. Kelly, E.A. Meulenkamp, Phys. Rev. Lett. 93 (2004) 166.
[46] C.D. Dimitrakopoulos, P.R.L. Malenfant, Adv. Mater. 14 (2002) 99.
[47] Z. Bao, A. Dodabalapur, A.J. Lovinger, Appl. Phys. Lett. 69 (1996) 4108.
[48] M.J. Panzer, C.D. Frisbie, Appl. Phys. Lett. 88 (2006) 203504.
[49] J. Takeya, K. Yamada, K.K. Shigeto, K. Tsukagoshi, S. Ikehata, Y. Aoyagi, Appl. Phys. Lett. 88 (2006) 112102.
[50] H. Shimotani, H. Asanuma, J. Takeya, Y. Iwasa, Appl. Phys. Lett. 89 (2006) 203501.
[51] M.J. Panzer, C.D. Frisbie, J. Am. Chem. Soc. 127 (2005) 6960.
[52] A.S. Dhoot, J.D. Yuen, M. Heeney, I. McCulloch, D. Moses, A.J. Heeger, Proc. Natl. Acad. Sci. USA 103 (2006) 11834.
[53] T. Ozel, A. Gaur, J.A. Rogers, M. Shim, Nano Lett. 5 (2005) 905.
[54] E.W. Paul, J.W. Thackeray, M.S. Wrighton, J. Phys. Chem. 90 (1986) 6080.
[55] S. Chao, M.S. Wrighton, J. Am. Chem. Soc. 109 (1987) 6627.
[56] S. Chao, M.S. Wrighton, J. Am. Chem. Soc. 109 (1987) 2197.
[57] P. Bergveld, IEEE Trans. Biomed. Eng 17 (1970) 70.
[58] Q. Pei, G. Yu, C. Zhang, Y. Yang, A.J. Heeger, Science 269 (1995) 1086.
[59] J. Gao, G. Yu, A.J. Heeger, Appl. Phys. Lett. 71 (1997) 1293.
[60] G. Yu, Y. Cao, C. Zhang, Y.F. Li, J. Gao, A.J. Heeger, Appl. Phys. Lett. 73 (1998) 111.
[61] Q. Pei, A.J. Heeger, Nat. Mater. 7 (2008) 167.
[62] P. Matyba, K. Maturova, M. Kemerink, N.D. Robinson, L. Edman, Nat. Mater. 8 (2009) 672.
[63] A.J. Heeger, N.S. Sariciftci, E.B. Namdas, Semiconducting and Metallic Polymers, Oxford University Press Inc., New York, 2010.
[64] A. Hepp, H. Heil, R. Schmechel, H. von Seggern, Adv. Eng. Mater. 7 (2005) 957.
[65] C. Yumusak, N.S. Sariciftci, Appl. Phys. Lett. 97 (2010) 033302.
[66] B. Liu, G.C. Bazan, Chem. Mater. 16 (2004) 4467.
[67] M. Hara, Polyelectrolytes: Science and Technology, Marcel Dekker, New York, 1993.
[68] M.R. Pinto, K.S. Schanze, Synthesis (Mass) 9 (2002) 1293.
[69] S.M. Sze, Physics of Semiconductor Devices, 3rd ed., Wiley, New York, 2007.